

# Low-cost FBG temperature sensor for application in cultural heritage preservation

I. IVAȘCU<sup>a,\*</sup>, D. TOSI<sup>b</sup>, M. OLIVERO<sup>b</sup>, G. PERRONE<sup>b</sup>, N. N. PUȘCAȘ<sup>a</sup>

<sup>a</sup>University "Politehnica" Bucharest, Physics Department, Splaiul Independentei, 313, 060042, Bucharest, Romania

<sup>b</sup>Politecnico di Torino, PhotonLab & Department of Electronics, C.so Duca degli Abruzzi, 24, 10129, Torino, Italy

In this paper we present a low-cost system for temperature measurement based on a fibre Bragg grating and a narrow bandwidth fixed-wavelength laser. The system has been calibrated in the range 7 °C ÷ 29 °C, and tested in outdoor conditions, exhibiting a maximum uncertainty of 1 °C over a 3 days. This performance, together with features such as small form factor and intrinsic fire safety, makes it a possible solution for continuous monitoring of cultural heritage infrastructures and artifacts.

(Received March 19, 2008; accepted April 2, 2008)

*Keywords:* Fibre optic sensor (FOS), Fibre Bragg grating (FBG), Bragg wavelength, Intensity modulation, Temperature sensor

## 1. Introduction

Fibre optic sensors (FOS) are particularly attractive for applications where the impossibility to start fires is of primary concern, such as in cultural heritage preservation. Optical fibres are intrinsically safe thanks to the absence of electrical signals and, since the same fibre can be used both for sensing and for transmitting the measurement data, they allow the interrogating electronics to be located in a safe site. Other advantages of FOS with respect to conventional sensors include: flexibility, low losses, immunity from electromagnetic interference and reduced weight/dimensions [1-6].

Among different approaches for sensing with optical fibres, fibre Bragg grating (FBG) sensors are often employed to measure strain and temperature, since they bring extra benefits such as: intrinsic sensor element integrated into the fibre, no moving parts, high sensitivity and wide operating range, multi-point sensing capabilities [2-4].

All these interesting properties, together with a low invasive impact, make the FBG the ideal candidate to monitor the conservation temperature of artifacts in museums, as targeted in this paper. However, the currently available commercial interrogation systems for FBG are quite expensive, limiting the use of these sensors in renowned and economically supported applications, thus preventing their widespread diffusion.

The usual means for interrogation of a FBG sensor are based on the detection of a narrowband signal backreflected by the sensor when excited with a broadband source, the so called Bragg wavelength. The Bragg wavelength shifts in response to a mechanical or a thermal stress, hence enabling the sensing capability. The detection system for measuring the Bragg wavelength may be a simple miniaturized spectrometer with a CCD readout, a passive optical filter, a tunable filter (e.g. Fabry-Perot) or an interferometric detection system. In many practical

cases, these techniques present some drawbacks because they involve complex devices with fine-mechanics moving parts, which raise costs and can fail in harsh environments [6].

To overcome these limitations, in this paper we present the realization and characterization of a low-cost and small form-factor FBG-based temperature sensor devised for continuous monitoring of artifacts and cultural heritage infrastructures. The sensing system presents a reduced complexity since it only makes use of a laser as light source, a photodiode as signal receiver and limited electronics for acquisition/processing.

The paper is organized as follows: in Sect. 2 we present some theoretical considerations concerning the behavior of the FBG sensor, in Sect. 3 the experimental setup together with relevant results and in Sect. 4 we draw the conclusions of this work.

## 2. Theoretical considerations

A fibre Bragg grating (FBG) consists of a periodic perturbation of the refractive index in a single-mode fibre, induced by exposure of the core to an intense optical UV interference pattern. The FBG acts as a stop-band filter, i.e. when excited by a broadband source it is transparent to all wavelengths but the Bragg wavelength  $\lambda_B$ , given by [2]:

$$\lambda_B = 2n_{eff}\Lambda \quad (1)$$

where  $n_{eff}$  is the effective refractive index of the unperturbed mode in the fibre and  $\Lambda$  represents the grating pitch. Any physical influence on the optical fibre, such as strain or temperature, leads to the variation of the refractive index or of the grating pitch with subsequent change in the Bragg wavelength [1-3].

By differentiating Eq. (1), the dependence of the Bragg wavelength on temperature can be expressed as:

$$\Delta\lambda_B = \left\{ \left( \frac{\partial\Lambda}{\partial T} \right) \frac{1}{\Lambda} + \left( \frac{\partial n_{eff}}{\partial T} \right) \frac{1}{n_{eff}} \right\} \lambda_B \Delta T \quad (2)$$

where  $\Delta\lambda_B$  is the Bragg wavelength shift corresponding to a temperature variation  $\Delta T$ . The first part of this equation relates to the thermal expansion of the fibre, whereas the second term is due to the thermal dependence of the refractive index. In silica fibres, the latter is the dominant effect, accounting for  $\sim 95\%$  of the observed wavelength shift [1].

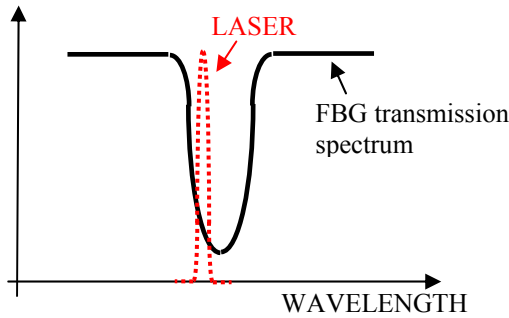


Fig. 1. The principle of FBG interrogation.

Since the transmitted spectrum of the FBG shifts under influence of the sensing parameter without changing its shape we exploited the possibility to interrogate the FBG sensor with a narrow-band laser source that has a fixed emission wavelength nearly matched with the FBG spectrum (Fig. 1). Therefore the transmitted power is modulated by the Bragg wavelength shift and its variation can be used to retrieve the temperature information.

### 3. Measurement setup and experimental results

The schematic design of the FBG sensor is presented in Fig. 2. A laser diode controller (LDC) provides the driving current to a laser diode which, in our experiments, is chosen to be a low-cost distributed feedback (DFB) laser for telecom applications packaged in a convenient butterfly case. An isolator between the laser source and FBG element reduces the reflected light from FBG which would be otherwise backscattered into the laser cavity, hence producing undesirable power fluctuations (self-mixing phenomena [7]). The optical signal transmitted through the FBG sensor element is detected by a photodiode which converts the optical power into a voltage. The photodiode voltage is then acquired by a personal computer (PC) by a National Instruments digital acquisition card 6036 (AC). A LabVIEW program was developed to control the acquisition process and subsequently derive the temperature estimation from the acquired data. The laser diode controller (LED - ILX Light-wave LDC-3722) allows changing the power and

the wavelength of the laser emission; the power being changed by varying the pump current and the wavelength trimmed by varying the temperature of the thermo-electrical controller (TEC). The current realization of the setup consists of cumbersome equipments, devised for lab experiments, but it can be easily miniaturized using microcontroller-based electronic boards.

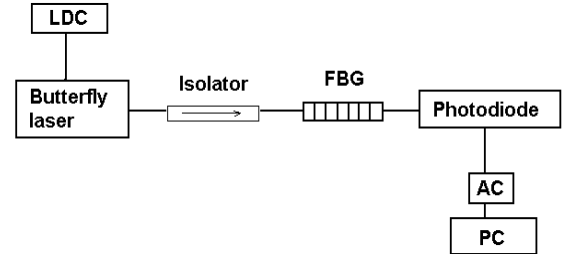


Fig. 2. FBG sensor arrangement; LDC – laser diode controller, FBG – fibre Bragg grating, AC – acquisition card, PC – personal computer.

All FBGs employed in the experiments were fabricated at the laboratory facilities of Politecnico di Torino. Each FBG was inscribed in a photosensitive single mode fibre with the phase mask technique [8], using an Argon-ions laser operating at 244 nm. The phase mask pitch was chosen to yield a Bragg wavelength  $\lambda_B$  close to 1560 nm. A typical reflected spectrum of the fabricated FBGs is presented in Fig. 3.

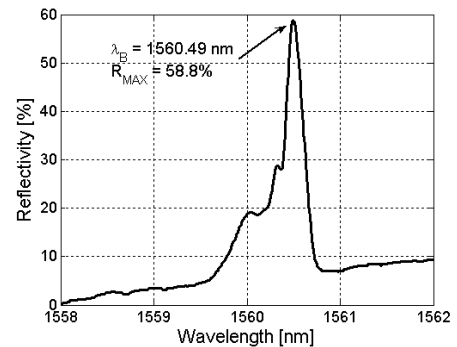


Fig. 3. Reflected spectrum of the FBG sensor.

**Laser stability.** Prior to employ the device into the detection scheme, we studied the long-term laser stability in order to assess its influence on the measure of temperature using the optical heterodyne technique, in which a signal wave of frequency  $f_s$  is mixed with a stable oscillator wave of frequency  $f_i$  using an optical coupler. The resulting beating signal oscillates at the frequency difference:

$$\Delta f_O = f_s - f_i \quad (3)$$

The experimental setup used for the study of the DBF laser frequency (wavelength) stability in time is presented

in Fig. 4. Following the heterodyne principle presented above, the DFB laser under test and an ultra-stable tunable laser were connected through a coupler 50/50. The mixed signal was split using a coupler 90/10. The 10%-arm was connected to an optical spectrum analyzer (OSA) to monitor the individual signals and to tune them at close frequencies. The second arm of the coupler was connected to a high-sensitivity photodiode (light-wave converter HP11982A) probed by an electrical spectrum analyzer (ESA).

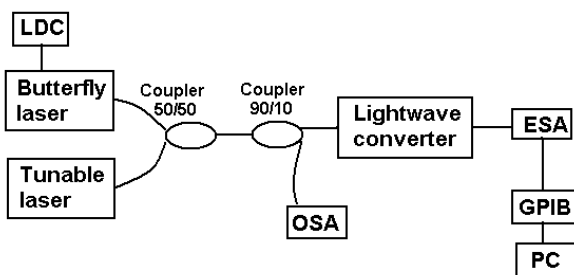


Fig. 4. Schematic of the setup used for studying the Butterfly laser frequency stability in time; LDC – laser diode controller, OSA – optical spectrum analyzer, ESA – electrical spectrum analyzer, GPIB – controller for High speed USB, PC – personal computer.

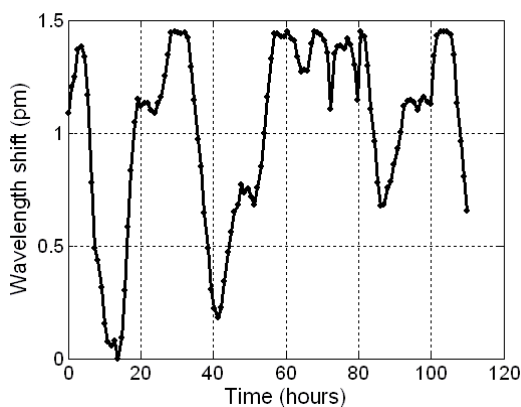


Fig. 5. The difference in wavelength between emission Butterfly laser and tunable laser vs time.

The laser under test was supplied with a current  $I = 57$  mA and its temperature was kept stable at  $30$  °C, corresponding to an emission wavelength of  $1560.248$  nm registered by the OSA. The result of the laser stability characterization is depicted in Fig. 5 where the wavelength shift is plotted as a function of time. Over a measurement time of  $110$  h the recorded maximum beat frequency variation was  $180$  MHz, equivalent to a maximum drift  $\Delta\lambda = 1.46$  pm that corresponds to  $\sim 1$  ppm of the nominal wavelength.

The study of the laser power stability was conducted by directly tracking the output of the laser with a high accuracy power meter (Agilent 8153A). As shown in Fig.

6, a power variation of  $4.3$   $\mu$ W ( $\sim 0.4\%$ ) over  $45$  h is observed.

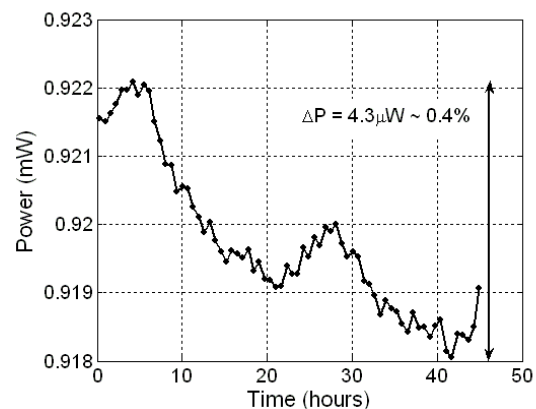


Fig. 6. The Butterfly laser emission power vs time.

In conclusion, the results of the laser stability characterization presented above highlight a wavelength variation of  $1$  ppm over  $100$  h and a power variation  $\sim 0.4\%$  in  $45$  h. Assuming a rule-of-thumb limit of  $1\%$  for any source of uncertainty in the sensor arrangement, the DFB laser has proved to have a good power/wavelength stability to be successfully employed in the temperature sensor arrangement.

*Calibration curve and sensor repeatability.* The sensor calibration curve, i.e. temperature vs photodiode voltage  $V$ , was obtained using the arrangement of Fig. 7, which resembles that of Fig. 2, though here the FBG is housed into a climatic chamber to perform temperature sweeps. An integrated circuit (IC) temperature sensor, type LM35 (absolute accuracy  $\leq 0.8$  °C [9]), is employed as a reference. The temperature reading from the LM35 and the signal from the photodiode are acquired on the same PC and processed with the LabVIEW program, here modified to handle multiple channels.

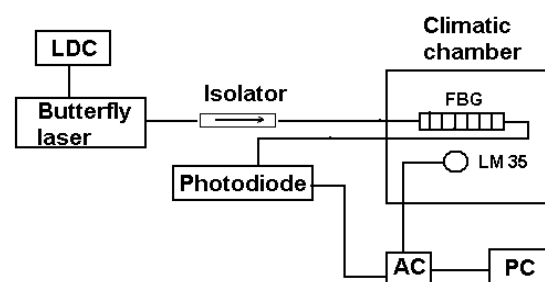


Fig. 7. The setup used for achieving of the sensor calibration curve; LDC – laser diode controller, FBG – fibre Bragg grating, LM35 – integrator, AC – acquisition card, PC – personal computer.

Once the calibration curve was defined, the LabVIEW acquisition program was extended to yield the temperature information, based on the acquired voltage from the photodiode.

In the experiments hereby presented, the laser temperature was set to 21 °C, and the device pumped with a current  $I = 150$  mA; the climatic chamber was programmed to run a cycle of increasing/decreasing temperature between 5 °C ÷ 35 °C over 3 h. The useful temperature range resulted to be restricted to the range 7 °C ÷ 29 °C, where the relationship temperature vs voltage is monotone. However that range is only limited by the FBG spectral bandwidth and could be easily extended by proper design of the FBG index profile [10].

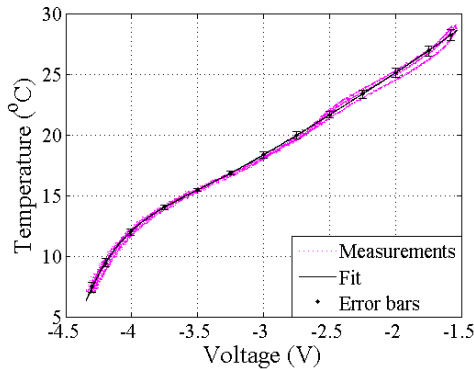


Fig. 8. The calibration curve of the temperature sensor.

The calibration curve must be repeatable over time, otherwise the reading of the sensor will be wrong. We performed a repeatability test by running three cycles where the temperature was swept from 5 °C to 35 °C and the experimental data were fitted with a 9<sup>th</sup> order polynomial function that would serve as a mean calibration curve for the subsequent experiments. Fig. 8 shows the experimental data (pink dots) together with the mean calibration curve (dark line). The large number of data collected during the three cycles, enabled to evaluate the repeatability as standard deviation from the fitted curve, which resulted to be always within ~1.5 % of the reading. However, due to the non-linearity of the relationship voltage-temperature, the uncertainty of a single measure depends on the reading, as depicted by the error bars on Fig. 8. The range 12 °C ÷ 25 °C exhibits smaller error bars, hence it can be defined as a restricted, yet higher-accuracy, range.

*Temperature sensor test in the climatic chamber and outdoor conditions.* The aim of this measurement campaign was to test the system under working conditions, first in a controlled environment (the climatic chamber) and then in outdoor conditions.

A series of tests was performed in the climatic chamber, where the FBG sensor underwent several temperature cycles and its reading was compared to the reference. An example of such a characterization is shown in Fig. 9, where a cycle of 18 h with the ramps from 7 °C to 30 °C and temperature recorded every 30 s.

A good overlap of the temperature measured by the LM35 and that estimated by the FBG is observed: the maximum deviation between the two measures is below 0.2 °C all over the sensor range while, as expected, saturation occurs below 7 °C and above 29 °C.

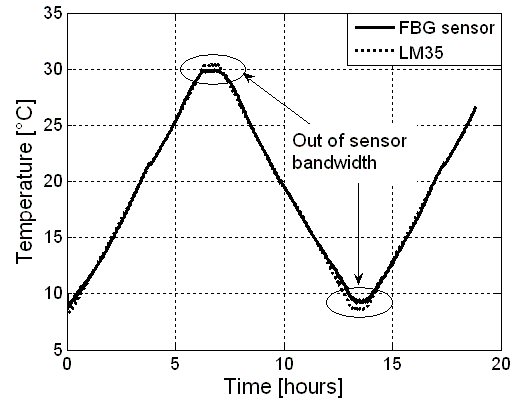


Fig. 9. Temperature measured by the FBG sensor and by LM 35, respectively vs. time.

A limitation of the system here presented is that the sensor reading changes if the attenuation along the light path changes, e.g. an extra fibre span is inserted between the FBG and the laser to reach far-away measurement spots hence introducing additional coupling/propagation losses. Such a drawback can be overcome, provided the calibration curve is scalable without distortion. We investigated such a possibility by introducing two fibre coils of 5 m along the laser-FBG path. The photodiode voltage was recorded with- ( $V$ ) and without- ( $V_0$ ) the extra fibre length and the scaling factor was calculated as  $\alpha = V/V_0$  and resulted to be  $\alpha = 1.32$ . The scaling factor was then used to recalibrate the V-°T curve for the new setup conditions, and the sensor tested once more in the climatic chamber. In the latter case ramps from 7 °C to 30 °C were applied over a total measurement time of 50 h.

The results are presented in Fig. 10, showing a good superposition between the temperature measured by the FBG sensor and the one measured by the LM35. The maximum difference, within 0.1 °C, confirms the successful power scalability of the sensor. Looking at a real environment application, this feature demonstrates the possibility to avoid an unpractical in-situ full calibration, exploiting instead a projection of a reference calibration curve previously measured in a lab framework.

Finally, experiments were carried out by placing the sensor outside for several days and recording the temperature readings. In order to strengthen the FBG against the harsh environmental conditions the FBG sensor was fastened on a metallic support and protected from rain while trying to preserve its sensing capability. In this case, the interrogation unit was placed inside the building.

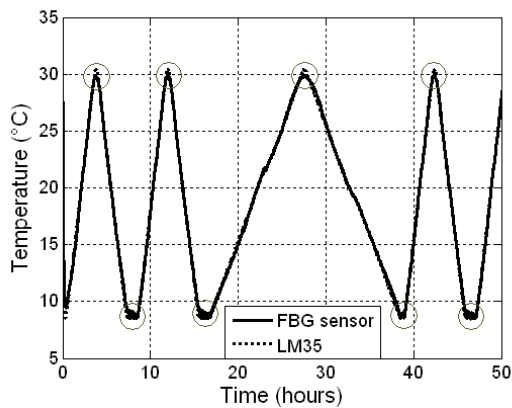


Fig. 10. The temperature measure by the FBG sensor and the LM 35, respectively vs. time after rescaling.

Two fibre spans of 5 m were used to connect the FBG to the control unit. The measurement lasted 70h, in which the temperature was recorded at a sampling interval of 8 min. The results, presented in Fig. 11, show a good correlation between the temperature measured by FBG sensor and the temperature read by LM35, with a maximum discrepancy of  $\sim 1^\circ\text{C}$ . The value, higher than that found within the climatic chamber and slightly outside the reference uncertainty, is likely to be attributable to the fact that the LM35 could not be positioned close enough to the FBG, and air circulation might have partially corrupted the comparison.

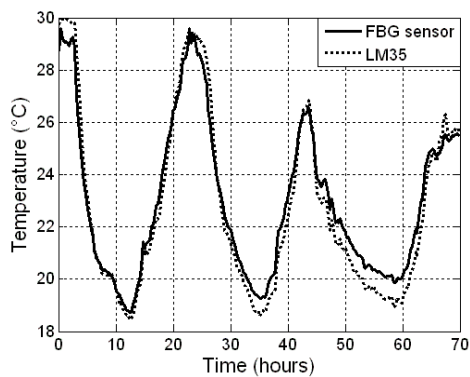


Fig. 11. The temperature measured by the FBG sensor and by LM 35, respectively, vs. time in outdoor conditions.

#### 4. Conclusions

This paper presents a low-cost temperature fibre Bragg grating sensor working in the range  $7^\circ\text{C} \div 29^\circ\text{C}$ , which can be further extended by proper design of the Bragg grating response. Contrary to other systems, in the presented arrangement the fibre Bragg grating is interrogated with a fixed-wavelength laser source and a photodiode, thus avoiding moving parts typical of the tunable lasers interrogation schemes, hence yielding a reliable, yet simple, measurement tool.

The off-the-shelf interrogation laser has been characterized in terms of wavelength/power stability, and it has proven to exhibit a good stability over a time frame of 3 days. The sensor behavior under controlled conditions, i.e. in a climatic chamber, exhibited a maximum offset of  $\sim 0.1^\circ\text{C}$  when compared, within controlled environment conditions, to a commercial integrated circuit temperature sensor model LM35.

The sensor test in outdoor conditions shows a maximum discrepancy of  $\sim 1^\circ\text{C}$ , the best working point being around the middle of the sensor range ( $12^\circ\text{C} \div 25^\circ\text{C}$ ). The presented sensor has been devised for civil engineering applications, with focus on the study of the temperature dynamics inside cracks.

#### References

- [1] P. K. Rastogi, *Optical Measurement Techniques and Applications*, Artech House, Inc. Boston, London, (1997).
- [2] K. O. Hill, G. Meltz, *Fiber Bragg Grating Technology Fundamentals and Overview*, *Journal of Lightwave Technology* **15**(8), 1263 (1997).
- [3] P. Ferraro, G. Natale, On the possible use of optical fiber Bragg gratings as strain sensors for geodynamical monitoring, *Optics and Lasers in Engineering* **37**, 115, (2002).
- [4] N. Takahashi, W. Thongnum, T. Ogawa, S. Tanaka, Compensation of Temperature-Induced Fluctuation in Fiber-Bragg-Grating Vibration Sensor by using Feedback Control of Source Wavelength, *Proceedings SBMO/IEEE MTT-S IMOC*, 2003, p.893.
- [5] B. Culshaw, *Optical Fiber Sensor Technologies: Opportunities and-Perhaps-Pitfalls*, *J. of Lightwave Technol.* **22**(1), 39 (2004).
- [6] D. Tosi, M. Olivero, G. Perrone, Broadband Source-Based Interrogation Scheme of Fiber Bragg Grating Sensors for Structural Health Monitoring, *Key engineering materials*, **347**, 399 (2007) <http://www.scientific.net/0-87849-444-8/5.html>
- [7] G. Giuliani, M. Norgia, S. Donati, T. Bosch, Laser diode self-mixing technique for sensing applications, *J. Opt. A: Pure Appl. Opt.* **4**, 283, (2002).
- [8] K. O. Hill, B. Malo, F. Bilodeau, D. C. Johnson, J. Albert, Bragg gratings fabricated in monomode photosensitive optical fiber by UV exposure through a phase mask, *Appl. Phys. Lett.*, **62**, 1035, (1993).
- [9] National Semiconductor, LM35 datasheet, <http://www.national.com>
- [10] J. Skaar, L. Wang, and T. Erdogan, "On the Synthesis of Fiber Bragg Gratings by Layer Peeling," *IEEE Journal of Quantum Electronics*, **37**, 165, (2001).

\*Corresponding author: [ivascu\\_ioana@physics.pub.ro](mailto:ivascu_ioana@physics.pub.ro)